UNIVERSITY OF NEW MEXICO
ALBUQUERQUE

ENGINEERING EXPERIMENT STATION

TECHNICAL REPORT EE-91

EXPERIMENTAL VERIFICATION OF THE INPUT IMPEDANCE OF THE COAXIAL UNDERSEA ANTENNA

by

VINCENT R. CHAVEZ
and
WILLIAM T. COWAN

July 1963

This work was performed
under Contract Nonr 2798(01)

Engineering Experiment Station

University of New Mexico

Albuquerque, New Mexico

Experimental Verification of the Input Impedance of the Coaxial Undersea Antenna

by

Vincent R. Chavez*

and

William T. Cowan†

*Presently with U. S. Armed Forces
Formerly, E. E. Department
University of New Mexico
Albuquerque, New Mexico

†E. E. Department
University of New Mexico
Albuquerque, New Mexico

This work was performed under
Contract Nonr 2798(01)

ABSTRACT

An experiment was performed to check the expressions for the impedance of a coaxial type of antenna submerged in a conducting medium (sea water). The experiment was conducted at high frequencies in order to take advantage of frequency scaling.

Details of the construction of the antenna along with methods and results of experimental measurements on the antenna are included.

The experimental results check closely with the theoretical values obtained using expressions derived on the assumption that the antenna in a conducting medium is considered a transmission line with a lossy outer conductor.

TABLE OF CONTENTS

LIST OF FIGURES

INTRODUCTION

The problem of radio wave propagation using antennas submerged in sea water has received much attention in recent years. As early as 1940, Norgorden [1][1] prepared a paper on the problem of propagation of radio waves from a transmitting antenna in air to a receiving loop antenna in sea water. Further work on the loop antenna was performed in 1946 by Quinn and Norgorden [2]. An analysis of a Hertzian dipole in an infinite, conducting medium was done by Tai [3] in 1947. He showed that a meaningful expression for the radiation resistance of the Hertzian dipole in a conducting medium can be obtained only if the dipole is insulated. Electric and magnetic dipoles in infinite and semi-infinite conducting media have been analyzed by several investigators since 1947; e.g., Moore [4], Lien [5], Baños and Wesley [6], Wait [7,8], and King [9]. Experimental work was done in 1960 by Kraichman [10] to verify the results of Wait and Baños, and by Saran and Held [11] to verify the exponential increase of attenuation with depth.

An extensive analysis of the submerged antenna problem was presented by Moore [4] in 1951. Moore analyzed the problem of the propagation of an electromagentic wave through sea water (a conducting medium), through the boundary between

---

[1]The numbers in brackets indicate the references in the bibliography.

the sea water and the air (a dielectric), and over the surface of the sea water. He treated the electric and magnetic dipoles in a conducting medium and analyzed three antenna configurations in this medium: the biconical antenna, the "coaxial antenna," and the small magnetic loop. In addition, Moore analyzed the power requirements for a system consisting of submerged sending and receiving antennas. The coaxial antenna had been analyzed theoretically and experimentally by Flath and Norgorden [12] in 1949 as a "lossy concentric line." However, this work was not available to Moore when he did his work. The results of these two independent investigations agree closely.

This paper reviews the analysis of the submerged coaxial antenna introduced by Flath and Norgorden and later independently by Moore. The theoretical review of the analysis is presented, followed by an experimental verification.

The derivation of the coaxial antenna input impedance in this report is based essentially on Moore's work. The purpose of the experiment which followed was to model the coaxial antenna for the lower frequencies when immersed in the sea. In order to represent the size of the sea adequately by a large tank which could be kept indoors, the antenna was scaled to operate in a frequency range from 75 to 125 mc./sec. All assumptions made in the theoretical analysis were investigated to insure that they would apply to the scaled model.

1. THE GENERAL SUBMERGED ANTENNA PROBLEM

An antenna submerged in sea water is much less efficient than the same antenna in air. This is due to the fact that the sea water has a much higher conductivity, and thus, forms a very lossy medium for the propagation of electromagnetic waves. The rate of attenuation can be determined for a plane wave in sea water by considering the propagation constant, γ_B, which is defined in terms of the electric field by

$$E = E_o e^{-(z\gamma_B - j\omega t)} \tag{1-1}$$

and is given by

$$\gamma_B = j\omega \sqrt{\mu \bar{\epsilon}} \tag{1-2}$$

where ω is the angular frequency, μ is the permeability of the medium, and $\bar{\epsilon}$ is the complex dielectric constant which is

$$\bar{\epsilon} = \epsilon + \frac{\sigma}{j\omega} \tag{1-3}$$

where ϵ is the real dielectric constant, and σ is the conductivity of the medium.

For sea water the complex dielectric constant is

$$\bar{\epsilon} = 7.17 \times 10^{-10} + \frac{\sigma}{j\omega} \tag{1-4}$$

It is apparent from this that for frequencies below 100 mc./sec. and for a conductivity of less than four mhos/meter,

$$\bar{\epsilon} \approx \frac{\sigma}{j\omega} \tag{1-5}$$

Substituting this value for $\bar{c}$ into expression (1-2) we obtain

$$\gamma_B = j\omega \sqrt{\frac{\mu\sigma}{j\omega}} = \sqrt{\frac{\omega\mu\sigma}{2}} (1 + j) . \qquad (1\text{-}6)$$

Thus, the wavelength in sea water becomes

$$\lambda = \frac{2\pi}{I_m \gamma_B} = 2\pi\sqrt{\frac{2}{\omega\mu\sigma}} . \qquad (1\text{-}7)$$

Where $I_m \gamma_B$ means the imaginary part of γ_B; the attenuation factor is

$$\alpha = \sqrt{\frac{\omega\mu\sigma}{2}} = \frac{2\pi}{\lambda} \qquad (1\text{-}8)$$

or in db

$$db = 20 \log_{10} e^{-\frac{2\pi}{\lambda}} = \frac{-40\pi}{\lambda} \log_{10} e = \frac{-55 \text{ db}}{\lambda} . \qquad (1\text{-}9)$$

Thus, the attenuation is inversely proportional to wavelength; and the distance of propagation through sea water for any given attenuation is proportional to the wavelength. This effect suggests the use of long wavelengths and, consequently, low frequencies, perhaps below 10 kc./sec. for full-scale practical communication systems.

The use of low frequencies requires that the submerged transmitting antenna be extremely large to be capable of transferring large amounts of power into the sea water. Large amounts of power radiated through the water require extremely high currents in the water because of its high conductivity. These currents must somehow be produced by the antenna. This fact makes the antenna an inherently low impedance device. The problem, then, is to design an antenna which has a sufficiently high driving point impedance without being excessively

large. A receiving antenna must also be large if it is to be reasonably sensitive at low frequencies.

Another factor to consider in the design of the antenna is the path of propagation. Several investigators[2] have found that the best path of propagation between two submerged antennas is: (a) propagation from the transmitting antenna directly to the surface; (b) propagation horizontally over the surface of the sea with some of the energy being refracted back into the sea; (c) propagation of the energy which is refracted downward from the surface toward the receiving antenna. This signal, which refracts into the water along the path of the surface wave, is the signal picked up by the receiving antenna. Thus, all signals, whether they are sea to sea, sea to air, or air to sea, are directed vertically to or from the submerged antenna. For maximum efficiency in transmitting or receiving a vertically directed wave, antennas must be used which produce horizontal fields.

---

[2] See for example Moore [4] p. 171, Williams [15] p. 44, Moore and Blair [16], and Anderson [13] p. 4.

2. THE COAXIAL ANTENNA

A very undesirable feature of a bare-wire antenna immersed in a conducting medium such as sea water is that most of the current fed to the antenna "leaks off" through the surrounding medium before it gets very far down the length of the antenna. A logical solution to this problem is to insulate the entire antenna. Such an insulated antenna can be analyzed as a coaxial transmission line whose outer conductor is the sea water. Because of the relatively poor outer conductor, the antenna looks like an extremely lossy transmission line whose outer conductor has a very large skin depth. The fields associated with this skin depth constitute the desired radiation into the water. Thus, the "loss" of this transmission line must be increased to increase the useful radiation.

The radiation or "loss" can be increased by terminating the line with either a short or an open circuit to maximize the standing wave ratio. The short circuit termination has been shown to be the most desirable [4, pp. 103, 137]. The simplest and most practical procedure that can be used to short the inner conductor to the sea water is to remove the insulation from a section at the end of the antenna leaving a quarter wavelength or more of the wire exposed to, and in contact with, the sea water. A better short circuit can be obtained by attaching a conducting plate or ball to the end of the antenna; however, such a structure has poor hydro-

dynamic properties and is undesirable as it hinders underwater mobility of the antenna.

In addition, insulating the antenna causes the effective current path to be longer than on an equivalent uninsulated antenna. The longer current path is desirable because it increases the effective length of the antenna. An increase in effective length of the antenna results in a larger driving point impedance. From a practical standpoint, it is desirable to have a driving-point impedance that can be easily matched to existing transmitting and receiving equipment. Also the magnitude of the dipole moment for a constant input power is larger.

2.1 Derivation of Impedance

In the theoretical analysis, the coaxial antenna is considered to be a perfectly circular cylinder surrounded by a coaxial dielectric sheath, which in turn is immersed in a highly conducting medium of infinite extent. Figure 2.1 illustrates two cross-sections of the coaxial antenna. Regions A and B are, respectively, the dielectric sheath and the sea water. Thus the subscripts A and B are used on all parameters in the following equations to indicate the region to which they pertain. The radius of the perfectly conducting inner cylinder and the outer radius of the dielectric sheath are designated as a and b, respectively. Cylindrical coordinates (r, Φ, z) are used, with the axis of the antenna coinciding with the z-axis.

Region B sea water, the outer conductor

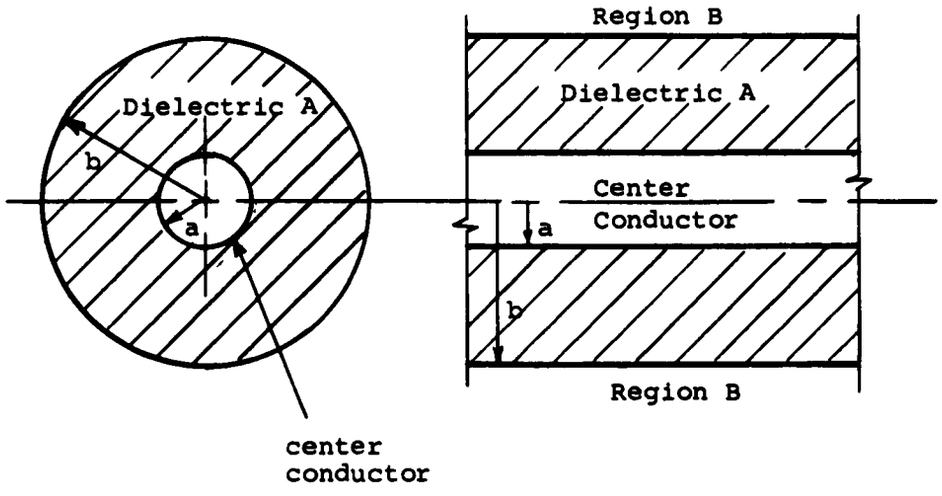

Figure 2.1 Cross section of the coaxial antenna.

For an antenna of practical dimensions the cutoff frequencies for any modes other than the transmission-line mode are much higher than the frequencies that are practical for communication in sea water. The transmission line mode requires a magnetic field component in the φ - direction (H_φ) and an electric field component in the r - direction (E_r). In addition, a longitudinal component of electric field (E_z) must exist due to the longitudinal voltage drop along the imperfect outer conductor. For perfect cylindrical symmetry these components are independent of φ, and there are no other field components.

To solve the boundary value problem for the field components we apply Maxwell's curl equations in Region B, the sea.

$$\nabla \times \vec{E} = - \frac{\partial \vec{B}}{\partial t} \tag{2-1}$$

$$\nabla \times \vec{H} = \sigma \vec{E} + \epsilon \frac{\partial \vec{E}}{\partial t} . \tag{2-2}$$

Assuming harmonic time variation and remembering that $\sigma >> \omega\epsilon$ in Region B gives

$$\nabla \times \vec{E} = - j\omega\vec{B} = - j\omega\mu\vec{H} \tag{2-3}$$

$$\nabla \times \vec{H} = \sigma \vec{E} . \tag{2-4}$$

Taking the curl of both sides of (2-3) using (2-4):

$$\nabla \times \nabla \times \vec{E} = - j\omega\mu\sigma\vec{E} . \tag{2-5}$$

Expanding the curl curl of $\vec{E}$ in cylindrical coordinates and keeping only those components which are present as dictated by the transmission line mode:

$$(\nabla \times \nabla \times \vec{E})_r = \frac{\partial^2 E_z}{\partial z \partial r} - \frac{\partial^2 E_r}{\partial z^2} \tag{2-6}$$

for a radial component and

$$(\nabla \times \nabla \times \vec{E})_z = \frac{\partial^2 E_r}{\partial r \partial z} - \frac{\partial^2 E_z}{\partial r^2} + \frac{1}{r}\frac{\partial E_r}{\partial z} - \frac{1}{r}\frac{\partial E_z}{\partial r} \tag{2-7}$$

for the longitudinal component.

As stated above, the mode which applies here in Region B is the transverse-magnetic, and this fact implies that the longitudinal variation is $e^{\pm\Gamma z}$, therefore the form of the assumed solution for the separation of variables method is:

$$\vec{E}(r,z) = \tilde{E}\, e^{\pm\Gamma z}\, \vec{a}_r + \hat{E}\, e^{\pm\Gamma z}\, \vec{a}_z , \tag{2-8}$$

where $\tilde{E}$ and $\hat{E}$ are arbitrary functions of r only, and Γ is the propagation constant for the "transmission line." The radial

component of (2-8) is the solution to (2-6) and the longitudinal component of (2-8) is the solution to (2-7).

Using (2-8) in (2-6) and (2-7) and taking the positive z direction:

$$(\nabla \times \nabla \times \vec{E})_r = - \Gamma \frac{\partial \hat{E}}{\partial r} e^{-\Gamma z} - \Gamma^2 \tilde{E} e^{-\Gamma z} \tag{2-9}$$

and

$$(\nabla \times \nabla \times \vec{E})_z = - \Gamma \frac{\partial \tilde{E}}{\partial r} e^{-\Gamma z} - \frac{\partial^2 \hat{E}}{\partial r^2} e^{-\Gamma z} - \frac{\Gamma}{r} \tilde{E} e^{-\Gamma z} - \frac{1}{r} \frac{\partial \hat{E}}{\partial r} e^{-\Gamma z}. \tag{2-10}$$

Equating the respective components of (2-5) to (2-9) and (2-10):

$$+ j\omega\mu\sigma E_r = \Gamma \frac{\partial \hat{E}}{\partial r} e^{-\Gamma z} + \Gamma^2 \tilde{E} e^{-\Gamma z} \tag{2-11}$$

$$+ j\omega\mu\sigma E_z = \Gamma \frac{\partial \tilde{E}}{\partial r} e^{-\Gamma z} + \frac{\partial^2 \hat{E}}{\partial r^2} e^{-\Gamma z} + \frac{\Gamma}{r} \tilde{E} e^{-\Gamma z} + \frac{1}{r} \frac{\partial \hat{E}}{\partial r} e^{-\Gamma z}. \tag{2-12}$$

But $E_r = \tilde{E} e^{-\Gamma z}$ and $E_z = \hat{E} e^{-\Gamma z}$. Then:

$$\tilde{E} = \frac{\partial \hat{E}}{\partial r} \frac{\Gamma}{j\omega\mu\sigma - \Gamma^2} \tag{2-13}$$

and

$$\frac{\partial^2 \hat{E}}{\partial r^2} + \frac{1}{r} \frac{\partial \hat{E}}{\partial r} + (k_B^2) \hat{E} = 0 \tag{2-14a}$$

where

$$k_B^2 = \Gamma^2 - j\omega\mu\sigma = \Gamma^2 - \gamma_B^2 . \tag{2-14b}$$

Equation (2-14a) has the solution

$$\hat{E} = E_o H_o^{(2)}(k_B r) \tag{2-15a}$$

and

$$E_{zB} = E_o H_o^{(2)}(k_B r) e^{-\Gamma z} \tag{2-15b}$$

where E_o is an arbitrary constant and $H_o^{(2)}(k_B r)$ is the Hankel function which satisfies the radiation condition.

Then E_r is easily found from (2-13) and (2-15a):

$$E_{r_B} = \frac{-E_o \Gamma}{k_B} H_o^{(2)'}(k_B r) e^{-\Gamma z} , \tag{2-16}$$

where the prime indicates the derivative with respect to r. Therefore the electric field vector is

$$\vec{E}_B = \frac{-E_o \Gamma H_o^{(2)'}(k_B r) e^{-\Gamma z}}{k_B} \vec{a}_r + E_o H_o^{(2)}(k_B r) e^{-\Gamma z} \vec{a}_z . \tag{2-17}$$

Now use (2-17) and (2-3) to find the H_{φ_B} field:

$$\frac{\nabla \times \vec{E}}{-j\omega\mu} = \vec{H}$$

$$H_{\varphi_B} = - \frac{\sigma E_o H_o^{(2)'}(k_B r) e^{-\Gamma z}}{k_B} \tag{2-18}$$

or

$$H_{\varphi_B} = \sigma E_o H_1^{(2)}(k_B r) e^{-\Gamma z} . \tag{2-19}$$

Thus we have found the general solutions for the electric and magnetic fields in region B, the sea.

Now we must find the fields in region A, the dielectric. Again, beginning with Maxwell's equations and assuming that the dielectric conductivity is zero and that the time variation is harmonic:

$$\nabla \times \nabla \times \vec{E} = \omega^2 \mu \epsilon \vec{E} . \tag{2-20}$$

Since the transmission line mode still applies, we have the same field components in the dielectric as were present in the sea.

Expanding the curl curl of $\vec{E}$ and assuming the longitudinal variation as $e^{\pm \Gamma z}$ as before we get the same z and r components as in (2-9) and (2-10). Equating these to the components of (2-20):

$$\omega^2\mu\epsilon E_r = -\Gamma \frac{\partial \hat{E}}{\partial r} e^{-\Gamma z} - \Gamma^2 \tilde{E} e^{-\Gamma z} \tag{2-21}$$

and

$$\omega^2\mu\epsilon E_z = -\Gamma \frac{\partial \tilde{E}}{\partial r} e^{-\Gamma z} - \frac{\partial^2 \hat{E}}{\partial r^2} e^{-\Gamma z} - \frac{\Gamma}{r} \tilde{E} e^{-\Gamma z} - \frac{1}{r} \frac{\partial \hat{E}}{\partial r} e^{-\Gamma z} . \tag{2-22}$$

And as before $E_r = \tilde{E}\, e^{-\Gamma z}$ and $E_z = \hat{E}\, e^{-\Gamma z}$ so

$$\tilde{E} = \frac{-\partial \hat{E}}{\partial r} \frac{\Gamma}{\Gamma^2 + \omega^2\mu\epsilon} , \tag{2-23}$$

which is similar to (2-13), and

$$\frac{\partial^2 \hat{E}}{\partial r^2} + \frac{1}{r} \frac{\partial \hat{E}}{\partial r} + (k_A^2)\hat{E} = 0 \tag{2-24a}$$

which is similar to (2-14a), where

$$k_A^2 = \Gamma^2 + \omega^2\mu\epsilon = \Gamma^2 + \gamma_A^2 . \tag{2-24b}$$

It is clear that (2-24a) is the Bessel equation and has solutions:

$$\hat{E}_A = A_1 J_o(k_A r) + A_2 N_o(k_A r) \tag{2-25}$$

and

$$\tilde{E}_A = [A_1 J_o'(k_A r) + A_2 N_o'(k_A r)] \frac{-\Gamma k_A}{\Gamma^2 + \omega^2\mu\epsilon} \tag{2-26}$$

or

$$\tilde{E}_A = \frac{-\Gamma}{k_A} [A_1 J_o'(k_A r) + A_2 N_o'(k_A r)] \tag{2-27}$$

and the electric field vector in region A, the dielectric is

$$\vec{E}_A = [A_1 J_o(k_A r) + A_2 N_o(k_A r)] e^{-\Gamma z} \vec{a}_z - \frac{\Gamma}{k_A} [A_1 J_o'(k_A r) + A_2 N_o'(k_A r)] e^{-\Gamma z} \vec{a}_r . \tag{2-28}$$

Applying the curl equation

$$\frac{\nabla \times \vec{E}}{-j\omega\mu} = \vec{H}$$

as before to find H_{φ_A}:

$$H_{\varphi_A} = \frac{1}{-j\omega\mu}\left[\frac{\Gamma^2}{k_A}\left(A_1 J_o'(k_A r) + A_2 N_o'(k_A r)\right)e^{-\Gamma z} - \left(k_A A_1 J_o'(k_A r) + k_A A_2 N_o'(k_A r)\right)e^{-\Gamma z}\right] \qquad (2\text{-}29)$$

or in a more compact form:

$$H_{\varphi_A} = -\frac{j\omega\epsilon\, e^{-\Gamma z}}{k_A}\left[A_1 J_o'(k_A r) + A_2 N_o'(k_A r)\right]. \qquad (2\text{-}30)$$

Thus we have the $\vec{E}$ and $\vec{H}$ fields in both regions.

Now the constants E_o, Γ, k_B, k_A, and the ratio of A_2/A_1 need to be determined from the boundary conditions. These conditions are:

$$E_{z_A}(a) = 0 \qquad (2\text{-}31a)$$

$$E_{z_A}(b) = E_{z_B}(b) \qquad (2\text{-}31b)$$

$$H_{\varphi_A}(b) = H_{\varphi_B}(b)\ . \qquad (2\text{-}31c)$$

One more condition is dictated by the assumed transmission line mode as

$$H_{\varphi_A}(r) = \frac{I}{2\pi r} \qquad (2\text{-}31d)$$

where $I = I_o e^{-\Gamma z}$ is the current in the center conductor.

Condition (2-31d) and (2-31c) are used to find E_o:

$$\sigma\, E_o H_1^{(2)}(k_B b)\, e^{-\Gamma z} = \frac{I_o e^{-\Gamma z}}{2\pi b}$$

$$E_o = \frac{I_o}{2\pi b\sigma\, H_1^{(2)}(k_B b)}\ . \qquad (2\text{-}32)$$

Applying (2-31c) again but with (2-30) and (2-18):

$$\frac{j\omega\epsilon}{k_A}\left[A_1 J_o'(k_A b) + A_2 N_o'(k_A b)\right] = \frac{\sigma}{k_B} E_o H_o^{(2)'}(k_B b) \quad , \qquad (2\text{-}33)$$

and applying (2-31b)

$$A_1 J_o(k_A b) + A_2 N_o(k_A b) = E_o H_o^{(2)}(k_B b) \quad . \qquad (2\text{-}34)$$

Dividing (2-34) by (2-33) and solving for $\frac{A_2}{A_1}$:

$$\frac{A_2}{A_1} = -\frac{J_o(k_A b) - \frac{jk_B\omega\epsilon}{\sigma k_A}\frac{H_o^{(2)}(k_B b)}{H_o^{(2)'}(k_B b)} J_o'(k_A b)}{N_o(k_A b) - \frac{jk_B\omega\epsilon}{\sigma k_A}\frac{H_o^{(2)}(k_B b)}{H_o^{(2)'}(k_B b)} N_o'(k_A b)} \quad , \qquad (2\text{-}35)$$

and from (2-31a)

$$\frac{A_2}{A_1} = -\frac{J_o(k_A a)}{N_o(k_A a)} \quad . \qquad (2\text{-}36)$$

Equating (2-36) and (2-35):

$$\frac{J_o(k_A a)}{N_o(k_A a)} = \frac{J_o(k_A b) - \frac{jk_B\omega\epsilon}{\sigma k_A}\frac{H_o^{(2)}(k_B b)}{H_o^{(2)'}(k_B b)} J_o'(k_A b)}{N_o(k_A b) - \frac{jk_B\omega\epsilon}{\sigma k_A}\frac{H_o^{(2)}(k_B b)}{H_o^{(2)'}(k_B b)} N_o'(k_A b)} \quad , \qquad (2\text{-}37a)$$

and equating (2-14b) and (2-24b) we have two equations involving k_A and k_B to solve simultaneously:

$$k_B^2 + j\omega\mu\sigma = k_A^2 - \omega^2\mu\epsilon \quad . \qquad (2\text{-}37b)$$

In order to avoid a trial and error or computer type solution, some approximations in k_A and k_B can be made such as the following:

$$|k_A a| << 1 \tag{2-38a}$$

$$|k_A b| << 1 \tag{2-38b}$$

$$|k_B b| << 1 \ . \tag{2-38c}$$

With these apprxomations the small argument values of the Bessel functions may be used; these are:

$$\begin{aligned} J_o(x) &\cong 1 \\ N_o(x) &\cong -\frac{2}{\pi} \ln \frac{2}{\gamma x} \\ J_o'(x) &= -\frac{x}{2} \\ N_o'(x) &\cong \frac{2}{\pi x} \\ H_o^{(2)}(x) &\cong 1 + j\frac{2}{\pi} \ln \frac{2}{\gamma x} \\ H_o^{(2)'}(x) &\cong -j\frac{2}{\pi x} \end{aligned} \tag{2-39}$$

where γ is Euler's constant (1.781...).

Substituting these approximations into (2-37a) gives:

$$\frac{-\pi}{2 \ln \frac{2}{\gamma k_A a}} = \frac{1 - \frac{\pi\omega\epsilon}{4\sigma}(k_B b)^2 (1 + j\frac{2}{\pi} \ln \frac{2}{\gamma k_B b})}{-\frac{2}{\pi} \ln \frac{2}{\gamma k_A b} + \frac{\omega\epsilon}{\sigma}\left[\frac{k_B}{k_A}\right]^2 (1 + j\frac{2}{\pi} \ln \frac{2}{\gamma k_B b})} \ . \tag{2-40}$$

Solving for k_A^2 and using (2-37b) gives:

$$k_B^2 + j\omega\mu\sigma + \omega^2\mu\epsilon = - \frac{\pi\omega\epsilon}{2\sigma \ln \frac{b}{a}} k_B^2 (1 + j\frac{2}{\pi} \ln \frac{2}{\gamma k_B b})(1 - \frac{(k_A b)^2}{2} \ln \frac{2}{\gamma k_A a}) \ . \tag{2-41}$$

In practical cases such as we are considering

$$\frac{\sigma}{\epsilon} >> \omega \tag{2-42}$$

and as Moore [4, p. 110] justifies for low frequencies

$$\frac{\pi\epsilon}{2\sigma \ln\frac{b}{a}} k_b^2\left(1 + j\frac{2}{\pi}\ln\frac{2}{\gamma k_B b}\right)\left(1 - \frac{(k_A b)^2}{2}\ln\frac{2}{\gamma k_A a}\right) << \mu\sigma \quad (2\text{-}43)$$

which implies that

$$k_B^2 \cong - j\omega\mu\sigma \ . \quad (2\text{-}44)$$

Substituting this value of k_B into (2-41) gives:

$$k_A^2 = \frac{j\pi\omega^2\epsilon\,\mu}{2 \ln\frac{b}{a}}\left[1 + j\frac{2}{\pi}\left(\ln\frac{2}{\gamma|\sqrt{j\omega\mu\sigma}\, b|} + j\frac{\pi}{4}\right)\right]\left[1 - \frac{k_A^2 b^2}{2}\ln\frac{2}{\gamma k_A a}\right]. \quad (2\text{-}45)$$

Then collecting k_A^2 terms:

$$k_A^2\left[1 + \frac{\omega^2\epsilon\,\mu b^2}{2 \ln\frac{b}{a}}\left(\ln\frac{2}{\gamma k_A a}\right)\left(\frac{\pi}{4} + j \ln\frac{2}{\gamma|\sqrt{j\omega\mu\sigma}\, b|}\right)\right] =$$

$$\frac{j\omega^2\epsilon\,\mu}{\ln\frac{b}{a}}\left[\frac{\pi}{4} + j \ln\frac{2}{\gamma|\sqrt{j\omega\mu\sigma}\ b|}\right] . \quad (2\text{-}46)$$

One final approximation which is easily met allows the evaluation of k_A^2, this is

$$\left|\frac{\omega^2\epsilon\,\mu b^2}{2 \ln\frac{b}{a}}\left(\ln\frac{2}{\gamma k_A a}\right)\left(\frac{\pi}{4} + j \ln\frac{2}{\gamma|\sqrt{j\omega\mu\sigma}\ b|}\right)\right| << 1 \ . \quad (2\text{-}47)$$

Thus (2-46) can be rewritten as:

$$k_A^2 \cong \frac{j\omega^2\mu\epsilon}{\ln\frac{b}{a}}\left[\frac{\pi}{4} + j \ln\frac{2}{\gamma|\sqrt{j\omega\mu\sigma}\ b|}\right] . \quad (2\text{-}48)$$

Now the value of the propagation constant along the line, Γ, can be found by applying (2-24b):

$$\Gamma^2 = \frac{\omega^2 \mu \epsilon}{\ln \frac{b}{a}} \left[j\frac{\pi}{4} - \ln \frac{2b}{a\gamma |k_B b|} \right] . \qquad (2\text{-}49)$$

Thus we have found the quantities which characterize this "lossy transmission line," or the coaxial antenna in the sea.

The characteristic impedance, Z_o, of any uniform transmission line such as our coaxial line can be expressed in terms of the propagation constant, Γ, and the admittance per unit length, y, as

$$Z_o = \frac{\Gamma}{y} . \qquad (2\text{-}50)$$

Since the dielectric of the coaxial antenna is assumed to be lossless the admittance becomes

$$y = j \frac{2\pi\omega\epsilon}{\ln \frac{b}{a}} \qquad (2\text{-}51)$$

as it would be for any coaxial line with a lossless dielectric. The characteristic impedance is, therefore,

$$Z_o = \frac{\Gamma \ln \frac{b}{a}}{j2\pi\omega\epsilon} . \qquad (2\text{-}52)$$

The driving point impedance for a short-circuited line of length, ℓ, is

$$Z_{sc} = Z_o \tanh \Gamma\ell = \frac{\Gamma \ln \frac{b}{a}}{j2\pi\omega\epsilon} \tanh \Gamma\ell . \qquad (2\text{-}53)$$

For short lengths, ℓ, such that $(\Gamma\ell) < \frac{\pi}{2}$, the hyperbolic tangent may be expanded in a power series. In actual practice for frequencies less than 20 kc. and antenna lengths ℓ smaller than 100 meters, only one term of the hyperbolic tangent series is required. However, for the modeled antenna lengths and the

VHF frequencies used for the model, four or more terms are required. Using the first term of the power series only:

$$Z_{sc} = \frac{\Gamma \ln \frac{b}{a}}{j2\pi\omega\epsilon} (\Gamma\ell) = \frac{\Gamma^2 \ell \ln \frac{b}{a}}{j2\pi\omega\epsilon} . \qquad (2\text{-}54)$$

Substituting in the value of Γ^2 given by equation (2-49), the input impedance becomes:

$$Z_{in} = \frac{\omega\mu\ell}{\delta} + j\left[\frac{\omega\mu\ell}{2\pi} \ln \frac{2b}{a\gamma|\sqrt{\omega\mu\sigma}\, b|}\right] . \qquad (2\text{-}55)$$

This is the theoretical value of input impedance of the practical submerged coaxial antenna; as the frequency of operation is increased, additional terms may be required for convergence of the hyperbolic tangent series.

2.2 Experimental Determination of the Impedance

An experiment was performed to determine the validity of the expressions for the impedance of the short-circuited coaxial antenna. The measurements were made using a small antenna, between 8 and 13 cm. in length, immersed in a tank of salt water 35 inches in diameter and containing a depth of 33 inches of water. Frequencies in the VHF range from 75 to 125 mc/sec. were used in order to obtain measurable impedance values. The experimental values were compared with the theoretical values obtained from (2-53), not (2-55). (See Appendix B for the derivation of the input impedance of the modeled antenna.) The theoretical values of input resistance and reactance of the model are shown in Figures 2.2 and 2.3, respectively.

Figure 2.2

Graphs of theoretical input resistance for the submerged coaxial antenna model for various antenna lengths vs. frequency.

Parameters used in the calculations were those of RG 142 U cable.

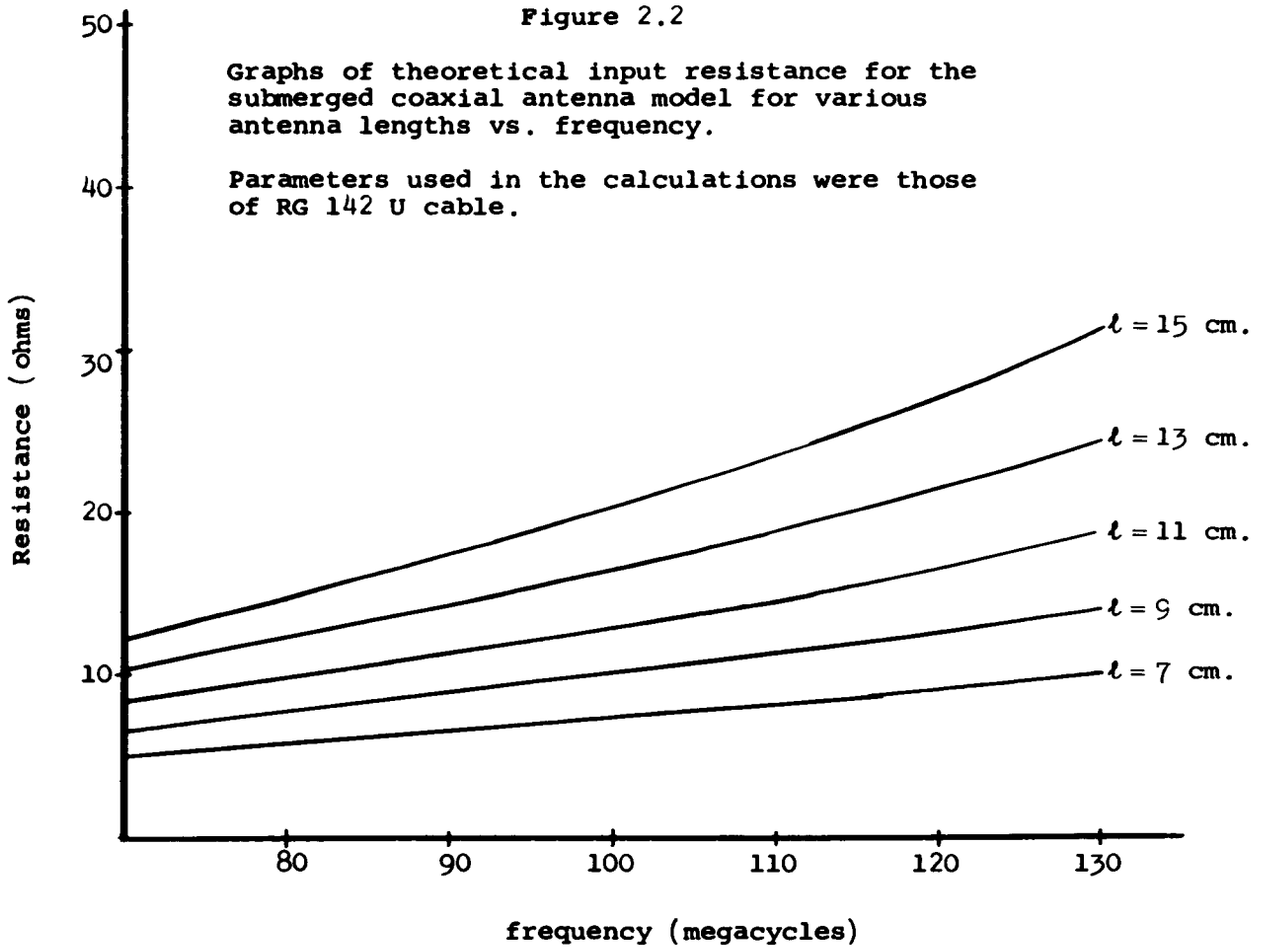

Figure 2.3

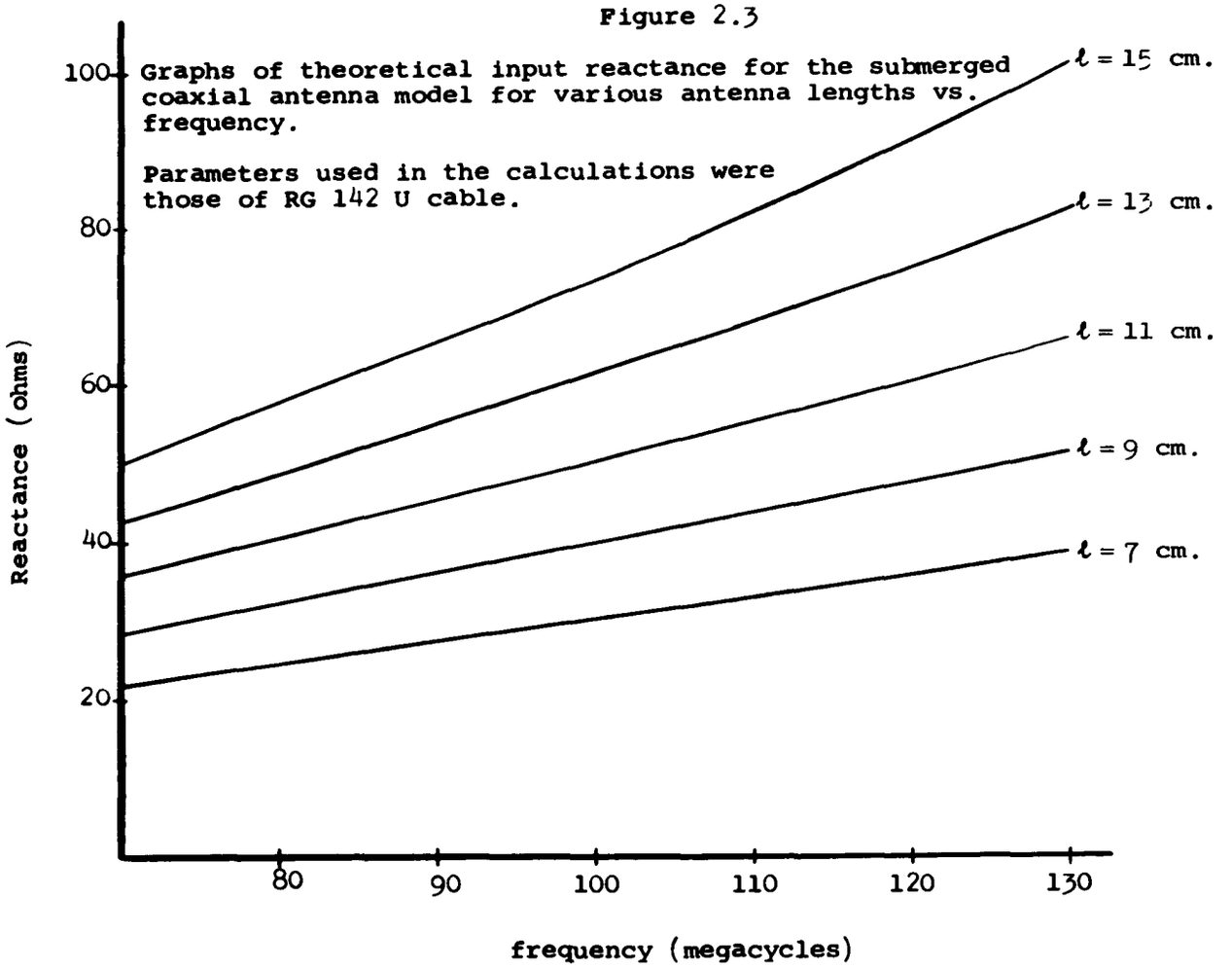
Graphs of theoretical input reactance for the submerged coaxial antenna model for various antenna lengths vs. frequency.
Parameters used in the calculations were those of RG 142 U cable.
ℓ = 15 cm.
ℓ = 13 cm.
ℓ = 11 cm.
ℓ = 9 cm.
ℓ = 7 cm.
Reactance (ohms)
100
80
60
40
20
80
90
100
110
120
130
frequency (megacycles)

The first antenna was made from RG 142 U coaxial cable by stripping back approximately 75 centimeters ($\ell + L_1$ + braid length) of the outer insulating jacket from the free end of the cable. Then a 21 centimeter length of the braid was removed from the same free end; next an 18 centimeter length of the teflon dielectric was removed exposing an equal length of the center conductor of the cable. Such an antenna is shown in Figure 2.4. Figure A.1 of the appendix shows how the antenna was placed in the water for the experiment. Shorter antennas were constructed by removing additional lengths of dielectric and center conductor. (See Figure A.3 of the appendix.) The diameters of the dielectric and the inner conductor of RG 142 U cable satisfy the conditions given by the inequalities (2-38).

When an antenna, described above, is submerged, a short circuit termination is obtained because of the relatively high conductivity of the salt water. The length L_1 was kept to at

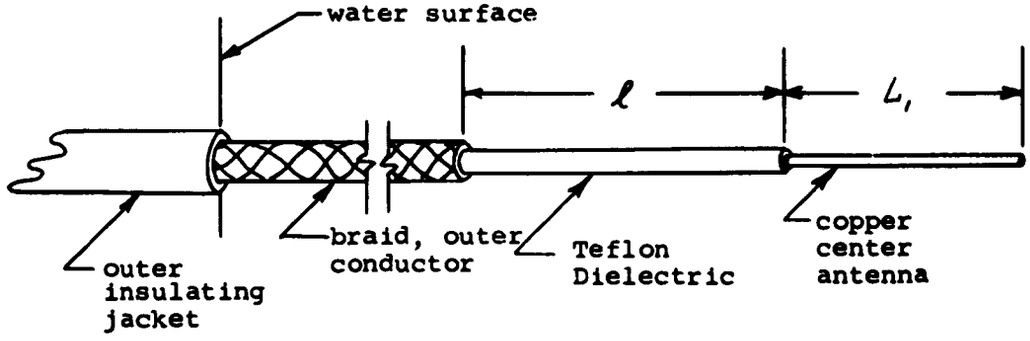

Figure 2.4 A coaxial antenna

least 18 cm. to insure that any reflections from the end of the bare wire were attenuated sufficiently and that their effect on the impedance was negligible.

The antenna was immersed in a salt water solution whose conductivity was approximately nine mhos/meter. The conductivity was measured with an ac. resistance bridge and a standard electrolytic cell employing platinum electrodes. The power supplied to the bridge was sixty cycle a.c. to prevent polarization of the electrodes.

The impedance measurements were made by means of a GR type 1602-B admittance meter using the necessary auxiliary General Radio equipment. The length of cable from the admittance meter to the coaxial antenna was about 18 inches. The length of this transmission line feeding the coaxial antennas had to be kept short to lower the effect of the cable losses on the antenna admittance measurements. That the losses are small is indicated by the negligible magnitude of the real part of the short circuit measurements. (Charts I and V of the appendix.) In order to compensate for this cable length, its electrical length had to be determined, and its effect removed from the antenna admittance data.

It was known that the electrical length of a transmission line could be determined from a short circuit admittance measurement made on the line. After the antenna admittance measurements had been completed, the transmission line which had fed the antennas was short circuited at the antenna feed point, and admittance measurements were made on it. These

short circuit measurements were made at every measurement frequency used for the antennas. (See the Appendix for frequencies and the method used to obtain the short circuit.)

The electrical wavelength of the line for each frequency was then determined from the Smith Chart. This frequency vs. wavelength data was then used to determine the "best straight line" relationship between frequency and wavelength according to the minimum error squared method shown in [21]. The corrected electrical wavelength for each frequency was then determined from the "best straight line" plot and used with the corresponding antenna input admittance measurement to determine the antenna input impedance.

The initial experimental curve of resistance versus frequency obtained with an antenna length of 13 cm. showed a higher resistance throughout the frequency range than was predicted from the theoretical curves. Subsequent measurements using other antenna lengths were also consistently higher, and there was no obvious reason from this discrepancy.

Since it was quite cumbersone to change antenna lengths and since the discrepancy at any antenna length seemed to be typical of the discrepancies at any other lengths, it was decided to make a more thorough investigation using only one antenna length. A length of 13 cm. was chosen for more detailed experimental study.

The experimental data plotted in Figure 2.5 indicates that the antenna behaves as though it is longer than its actual physical length; that is, there is an apparent electrical

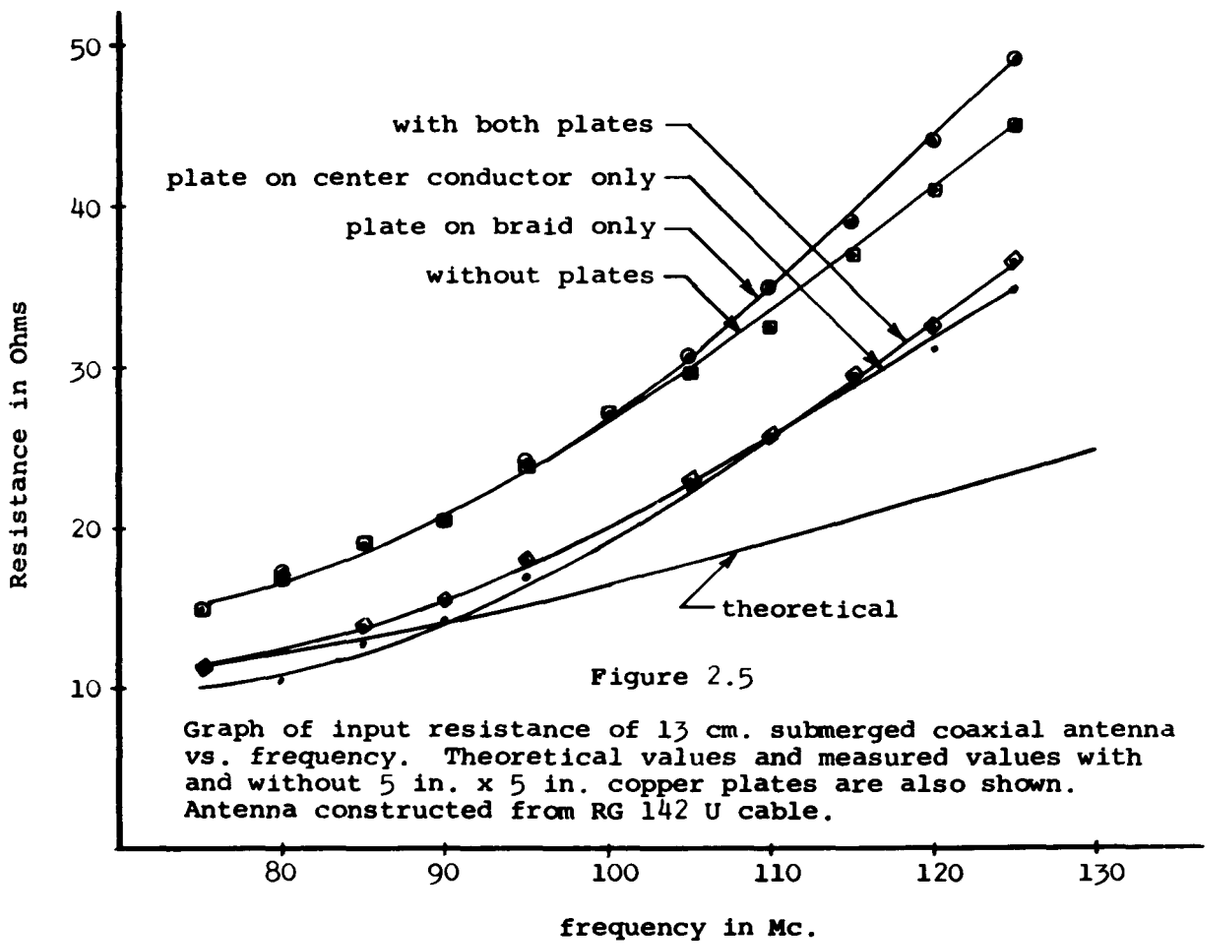

Figure 2.5

Graph of input resistance of 13 cm. submerged coaxial antenna vs. frequency. Theoretical values and measured values with and without 5 in. x 5 in. copper plates are also shown. Antenna constructed from RG 142 U cable.

length of the antenna which is greater than its measured physical length. The lengthening effect can be readily seen by comparing the experimental plot of the antenna resistance with the theoretical family of curves in Figure 2.2. A logical cause of this effect would seem to be the imperfect electrical contact between the salt water solution and the bare center conductor at the terminal end of the antenna and between the solution and the outer conductor of the cable at the driving point. In order to determine if this indeed was the cause for the discrepancy between theoretical and experimental values, additional surface area was added to both ends of the antenna in the form of metal plates (see Figure 2.6).

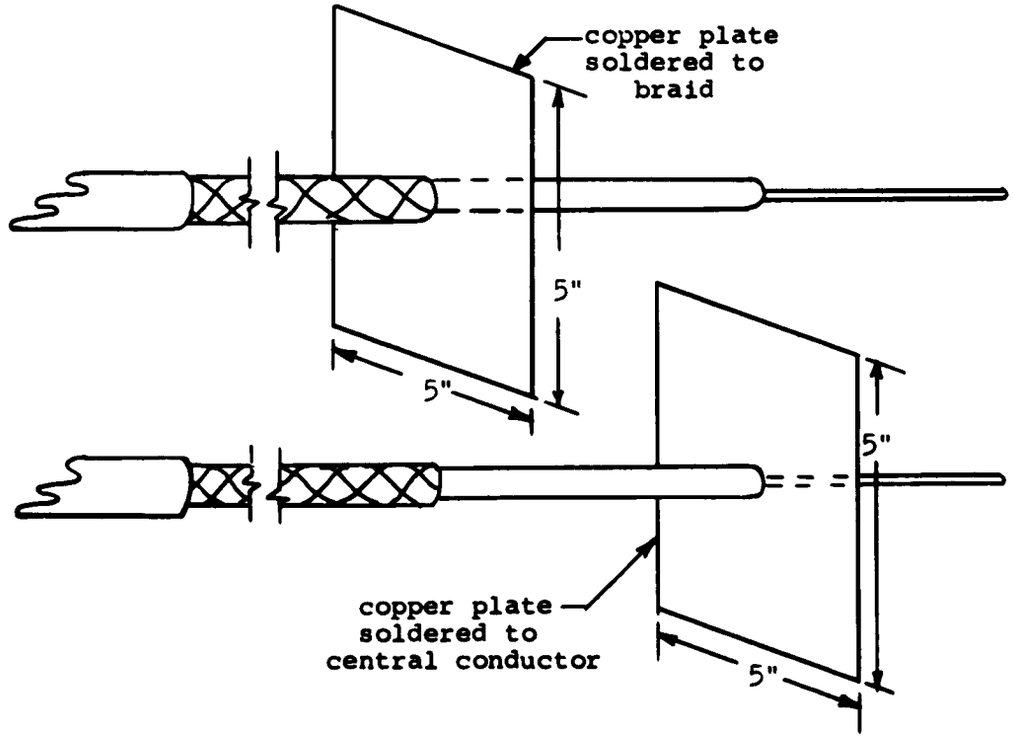

Figure 2.6 The coaxial antenna with metal plates.

A 5 in. x 5 in. metal plate was first soldered to the outer conductor of the cable to serve as a ground plane. This had negligible effect as shown in Figure 2.5. A similar ground plane soldered to the center conductor at the terminal end of the antenna proved effective in making the experimentally measured resistance agree closely with that predicted theoretically for the lower frequencies.

Figure 2.7 shows that the experimental points for the reactance follow the theoretical curve closely regardless of the presence of the ground planes. This effect is to be expected since most of the reactance is due to the magnetic field in the dielectric.

This experiment confirms the validity of the theory in spite of the discrepancies encountered between the theoretical values and the experimental values obtained for the coaxial antenna with no ground planes. This is true because the situation described in the theoretical analysis is more nearly like the situation represented by a coaxial antenna with ground planes at both ends. The theoretical analysis was based on an infinite line with all electric fields and currents oriented parallel to the line. The electric fields and currents between two large parallel plates perpendicular to the line are also parallel to the line. This is not true for a line terminated by bare wires coincident with the axis of the line, as is the case for the coaxial antenna without ground planes.

The current at either end of the coaxial antenna with no ground planes must flow in toward, or away from, the bare

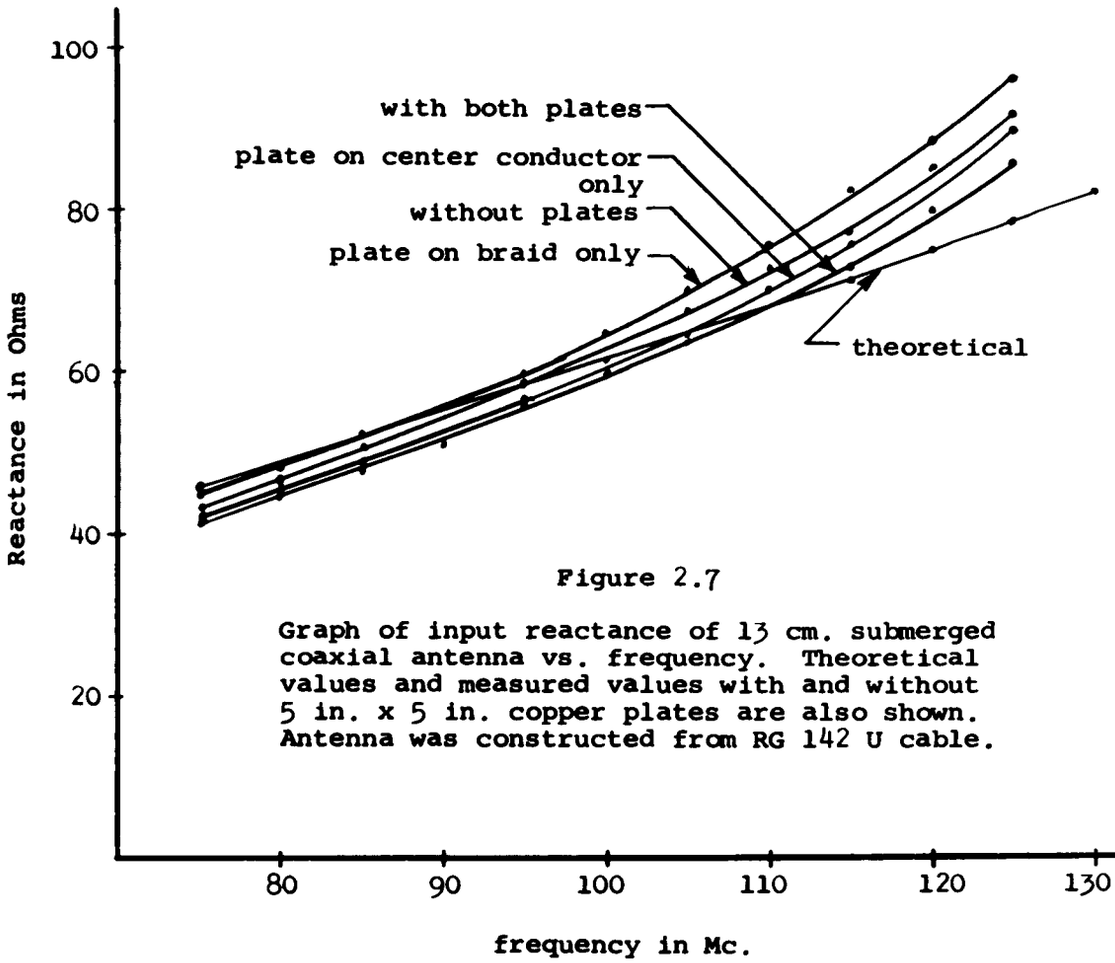

Figure 2.7

Graph of input reactance of 13 cm. submerged coaxial antenna vs. frequency. Theoretical values and measured values with and without 5 in. x 5 in. copper plates are also shown. Antenna was constructed from RG 142 U cable.

conductor. Because of the large skin depth as compared to the center conductor and comparatively low conductivity of the salt water solution, the current must be distributed over a large area of the bare conductor, and, thus, over an appreciable length of the conductor. This fringing effect increases the distance between the points where the current effectively enters and leaves the antenna. This increase in distance is more pronounced on the bare inner conductor at the terminal end than on the bare outer conductor at the driving point because the inner conductor has a smaller circumference than the outer conductor. Compared to the outer conductor with a larger circumference, the smaller circumference inner conductor must be longer to obtain the same contact area with the water. The truth of this statement is demonstrated by the fact that the ground plane at the terminal end of the antenna had a greater effect than the ground plane at the driving point.

Since a full scale practical antenna is necessarily extremely large, any phenomenon which makes the antenna appear to be larger than its actual size is desirable. For any given antenna length, the resistance is higher than expected from the theory, and, therefore, helps simplify the impedance matching problem. On the other hand, the increase in resistance is due mostly to losses at the terminal end, since, for a horizontal antenna, only the horizontal component of the fringing current contributes to the radiation at the water surface.

3. CONCLUSIONS

An antenna which operates well in air loses most of its effectiveness in sea water because electromagnetic waves traveling through the water are attenuated 55 db per wavelength. This makes it necessary to use low frequencies with corresponding long wavelengths to reduce the amount of attenuation for a given distance. The use of low frequencies requires very long antennas in order to keep the driving point impedance high enough to allow an effective transfer of power from a transmitter. Unfortunately, the efficiency of such an antenna is difficult to calculate since it is difficult to distinguish the useful power from the losses.

It should be noted that a full scale (low frequency) coaxial antenna with metal plates as described above would be impractical to build. Fairly good contact with the water can probably be provided at the driving end by the structure housing the transmitter, but good contact at the terminal end is difficult to obtain. The simplest way to do this would be to make a length of the center conductor bare at the terminal end. This method of shorting the antenna introduces some error as was shown by the experimental results presented above. An improvemert over this type of termination could be realized by increasing the diameter of the bare conductor; such an antenna is shown in Figure 3.1.

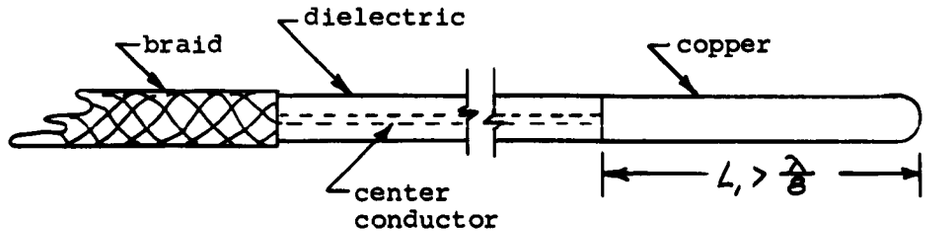

Figure 3.1 An improved coaxial antenna termination.

Due to the assumption that perfect contact with the water is assumed, the resistance of the coaxial antenna depends on the skin depth in the water and, thus, depends on the frequency [4, p. 116].

At the lower frequencies the measured resistance of the 13 cm. antenna agrees closely with theory. As the frequency increases, measured values depart somewhat from the calculated values. (See Figure 2.5.) Calculation of $|k_B b|$ at the higher frequencies shows that its value for the antenna used is less than 1, but not significantly so, as required by the inequality (2-38c). However, calculation will show that $|k_B b|$ can be much closer to 1 than (2-38c) implies. In general there is some doubt as to the validity of these calculations. This is because k_A and k_B are determined only after assumptions are made as to their magnitude.

When the more exact expression for k_A^2, [4, p. 110],

$$k_A^2 = \frac{j\omega\epsilon\, k_B}{\sigma\, b} \frac{H_o^{(2)}(k_B b)}{H_o^{(2)'}(k_B b)} \frac{1}{\ln \frac{b}{a}} \qquad (3\text{-}1)$$

was used to calculate k_A and then z_{in} at 125 mc., the value for the input impedance of the 13 cm. antenna at 125 mc was found to be

$$z_{in} = 122.1 + j\ 42.0 \text{ ohms.} \qquad (3\text{-}2)$$

While the resistive part is larger than the previously calculated resistance, as we would desire, it deviates more from the measured value than the less exact expression. The result also shows a greater divergence between the theoretical and measured reactance. This indicates that the more exact expression for k_A does not improve the agreement between the calculated and measured values. It appears then that the assumption that the coaxial antenna can be analyzed as a lossy transmission line may be invalid at the higher frequencies. At the lower frequencies, practical in underwater communications, the assumptions generally made in the analysis of coaxial antennas appear to be valid.

Some idea of the value of the impedance of a coaxial antenna of practical size can be gained by considering an antenna with the following dimensions.

$a = 0.5$ cm.

$b = 1.0$ cm.

$\ell = 10$ meters.

The impedance of this antenna operated at 10 kc. cylces/sec. in sea water with a conductivity of 4 mhos/meter is

$$Z \text{ input} = 0.0987 + j\ 0.775 \text{ ohms.} \qquad (3\text{-}3)$$

APPENDIX A

Experimental Procedure and Data

I. The Coaxial Antenna

1. Equipment
   (a) Tank filled with salt water
   Diameter: 34 inches
   Depth of water: 33 inches
   Gallons of water: Approximately 137
   Amount of salt in the water: Approximately 90 pounds
   (b) RG 142 U coaxial cable with outer conductor peeled back at the end to form the coaxial antenna.
   (c) 1 General Radio unit oscillator GR 1215 B Serial No. 2226
   (d) 1 General Radio unit oscillator GR 1215 B Serial No. 2047
   (e) 1 Hewlett Packard signal generator HP 608 C Serial 2083
   (f) 1 General Radio power supply GR 1201 B, USN No. 2798-3.
   (g) 1 General Radio intermediate frequency amplifier, GR 1216 A, USN No. 27987
   (h) 1 General Radio admittance meter with necessary attachments, GR 1602 B, Serial 2023
      (1) 1 General Radio standard conductance GS 1662 p4.
      (2) 1 General Radio standard capacitor GR 1602 p3, Serial 2023
      (3) 1 General Radio 20 cm. air line GR 874 L20
      (4) 1 General Radio low pass filter GR 874 F500
   (i) 2 General Radio 10 db attenuation pads GR 874 G10
   (j) 1 General Radio crystal mixer tee GR 874
   (k) 1 General Radio extension coaxial cable GR Co 874-R22
   (l) 1 Platinum electrode conductivity cell manufactured by Otto Haak's Son, Philadelphia 20, Pa.
   (m) 1 Leeds and Northrop Co. AC resistance bridge No. 761580-A
   (n) 1 0-100°C 76 mm thermometer.

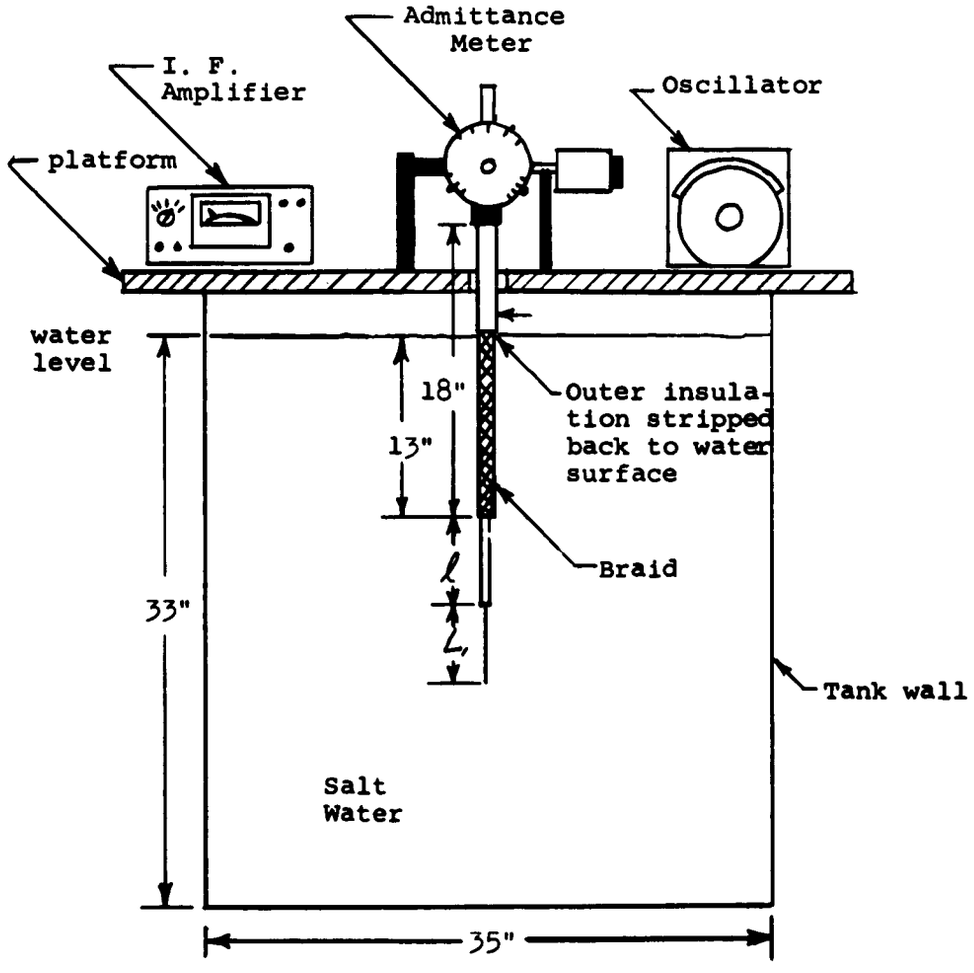

Figure A.1 Experimental setup.

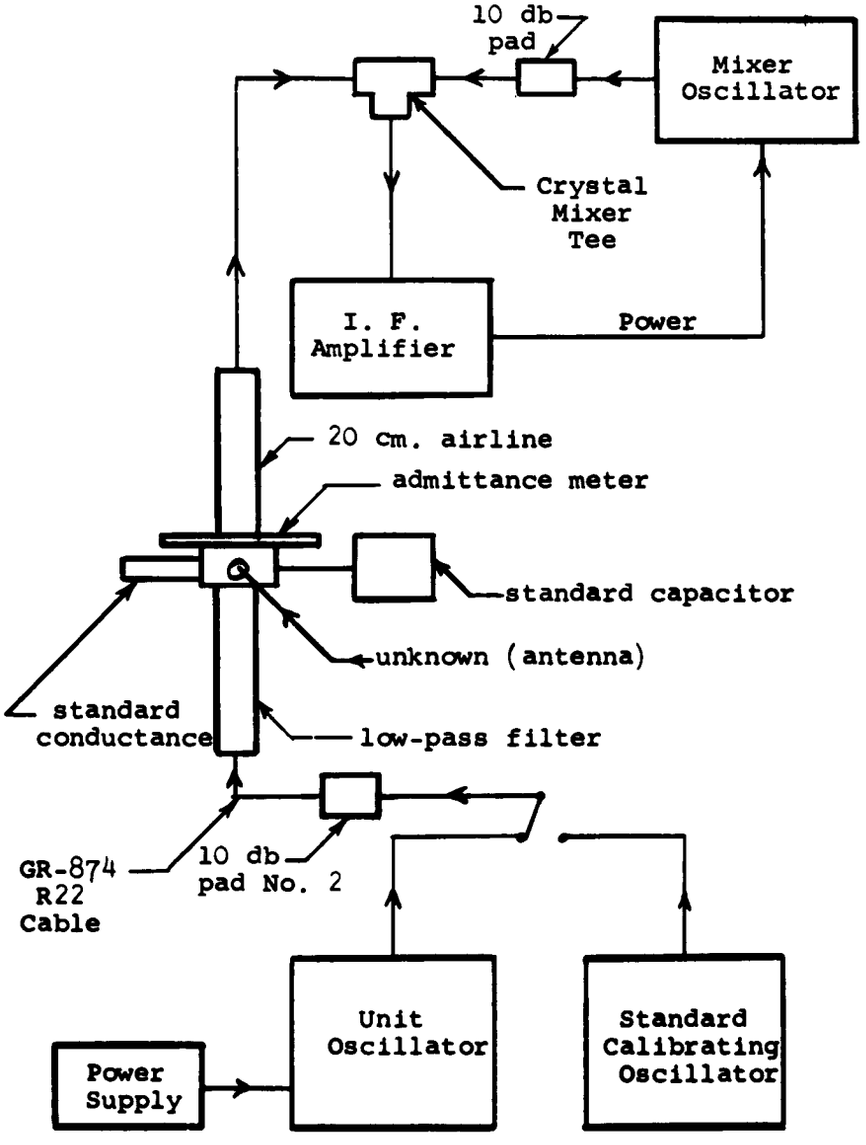

Figure A.2 Connection of measuring apparatus.

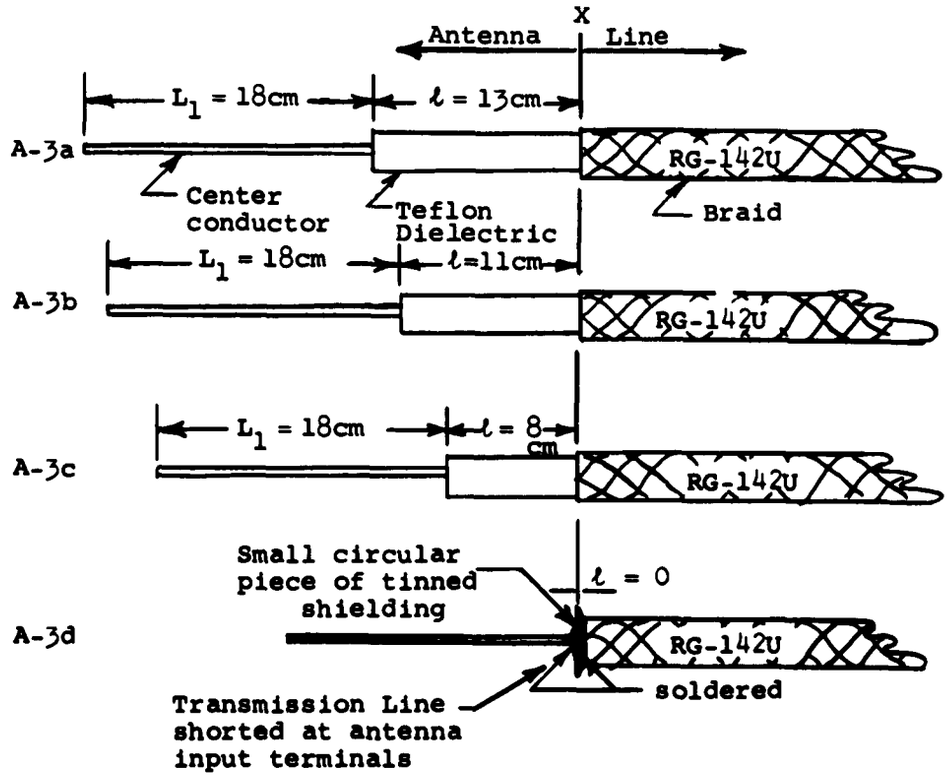

Figure A.3 Construction details of coaxial antennas and shorted transmission line.

II. Measurement Procedure

(a) The longest antenna (ℓ = 13 cm.) to be measured was first constructed from one end of a length of RG 142 U cable. (See Figure A.3a).

(b) Using a General Radio type 874 conductor, connection was made to the admittance meter as shown in Figure A.1.

(c) The frequency at which the measurement was to be made was set on the standard calibrating oscillator with the No. 2, 10 db pad connected to its output.

(d) The mixer oscillator was adjusted to a frequency approximately 30 mc. above the measurement frequency. Fine adjustment of mixer frequency was achieved by tuning for a maximum deflection of the IF amplifier output meter.

(e) The No. 2, 10 db pad was then disconnected from the standard calibrating oscillator and connected to the unit oscillator output.

(f) The unit oscillator frequency was set to the measurement frequency; then its frequency was carefully adjusted to maximum deflection of the IF amplifier output meter.

(g) With the standard capacitor set to the measurement frequency, the conductance and susceptance arms of the admittance meter were adjusted in turn until the IF amplifier output meter indicated a minimum null.

(h) Parts (c) through (g) were repeated for all desired measurement frequencies.

(i) The length ℓ was then shortened to the next longest antenna length. The length of bare center conductor was also shortened to 18 cm. (Figure A.3b)

(j) Steps (c) through (h) were repeated.

(k) ℓ was shortened to the next longest length ($\ell = 8$ cm.), and the bare center conductor length L_1 was adjusted to 18 cm. (Figure A.3c).

(l) Steps (c) through (h) were repeated.

III. Construction of Short Circuit for Determination of Line Length.

(a) The teflon dielectric was stripped back to the end of the braid. (Point X of Figure A.3a).

(b) A small piece of shielding was securely soldered to the center conductor and braid at X as shown in Figure A.3d.

(c) Measurement procedure steps (b) through (h) were repeated on this shorted transmission line.

IV. Experimental Data

Definitions:

f - measurement frequency.

λm - electrical wavelength determined from short circuited line measurements.

λc - electrical wavelength determined "best straight line" curve.

G - conductance measured at the input end of the transmission line with antenna load.

B - susceptance measured at the input end of the transmission line with antenna load.

G_s - conductance measured at the input end of the shorted transmission line.

B_s - susceptance measured at the input end of the shorted transmission line.

R - resistive component of antenna input impedance.

X - reactive component of antenna input impedance.

CHART I

Shorted transmission line

f MC	G_s Millimhos	B_s Millimhos	λ_m Per Unit	λ_c Per Unit
125	0	+5.5	.2925	.2925
120	0	+4.0	.2810	.2814
115	0	+2.55	.2700	.2703
110	0	+1.3	.2600	.2592
105	0	- .25	.2480	.2480
100	0	-1.55	.2375	.2369
95	0	-3.0	.2260	.2258
90	0	-4.5	.2140	.2147
85	0	-6.0	.2030	.2035
80	0	-7.5	.1920	.1924
75	0	-9.05	.1820	.1813

CHART II

ℓ = 13 cm. without plates
water temperature ~ 23° C
water conductivity ~ 9 mhos/m
line length determined from Chart I

f MC	G Millimhos	B Millimhos	R Ohms	X Ohms
125	56.4	52.5	42	+88.5
120	33.0	45.6	39.5	+80.0
115	21.0	37.35	35	+74.5
110	14.97	30.8	31	+69.5
105	10.8	25.2	27.5	+64.5
100	8.28	21.0	25	+61
95	6.45	17.0	21.5	+56.5
90	5.25	13.55	19.0	+52
85	4.5	10.9	17.5	+49
80	4.0	8.4	16	+46
75	3.55	6.0	15.8	+42.5

CHART III

ℓ = 11 cm. without plates
water temperature ~ 23° C
water conductivity ~ 9 mhos/m
line length determined from Chart I

f MC	G Millimhos	B Millimhos	R Ohms	X Ohms
125	31.2	+43.3	30	+67
120	20.2	+35.7	28.5	+63
115	14.4	+29.1	25.5	+58.5
110	10.8	+24.6	24.5	+55.5
105	8.4	+20.5	21.0	+52.0
100	6.6	+16.7	19.0	+48.8
95	5.5	+13.7	17.5	+46
90	4.6	+11	16	+43.3
85	4.05	+ 8.6	14.75	+40.7
80	3.8	+ 6.5	14.0	+38.5
75	3.4	+ 4.35	12.5	+36.5

CHART IV

ℓ = 8 cm. without plates
water temperature ~ 23°C
water conductivity ~ 9 mhos/m
line length determined from Chart I

f MC	G Millimhos	B Millimhos	R Ohms	X Ohms
125	15.2	+29.6	20	+46.3
120	11.4	+24.9	19	+44
115	9.01	+21.0	18	+41.5
110	7.2	+17.4	16.5	+39
105	5.95	+14.4	15	+36.8
100	4.95	+11.97	13.8	+35
95	4.3	+ 9.5	12.8	+33.5
90	3.75	+ 7.3	11.8	+31.5
85	3.5	+ 5.2	11.3	+29.5
80	3.35	+ 3.4	10.8	+28.5
75	3.0	+ 1.55	9.7	+27.3

CHART V

Shorted transmission line

f MC	G_s Millimhos	B_s Millimhos	λ_m Per Unit	λ_c Per Unit
125	.25	+5.5	.2928	.2924
120	.2	+4	.2813	.2813
115	0	+2.55	.2700	.2702
110	0	+1.2	.2593	.2591
105	0	- .25	.2480	.2480
100	0	-1.7	.2362	.2369
95	0	-3.05	.2258	.2258
90	0	-4.45	.2150	.2147
85	0	-6	.2031	.2036
80	0	-7.7	.1927	.1925
75	0	-9.1	.1818	.1815

CHART VI

ℓ = 13 cm. without plates
water temperature ~ 21° C
water conductivity ~ 7 mhos/m
line length determined from Chart V

f MC	G Millimhos	B Millimhos	R Ohms	X Ohms
125	62.0	+53.2	45	+92
120	36.3	+48.0	41	+85
115	23.1	+39.3	37	+77.5
110	15.8	+32.5	32.5	+73.0
105	11.4	+26.7	29.5	+68
100	8.76	+22.2	27	+64.5
95	6.95	+17.8	24	+59
90	5.55	+14.3	20.3	+54.5
85	4.8	+11.4	19	+51.0
80	4.2	+ 8.8	17.3	+47.0
75	3.65	+ 6.4	15	+43.8

CHART VII

ℓ = 13 cm. with 5 in. x 5 in.
copper plate soldered to the
end of the braid
water temperature ~ 21°C
water conductivity ~ 7 mhos/m
line length determined from Chart V

f MC	G Millimhos	B Millimhos	R Ohms	X Ohms
125	70.4	+53.2	49	+96
120	39.8	+50.1	44	+88.5
115	24.3	+41.1	39	+82.5
110	16.5	+33.9	35	+75.5
105	11.85	+27.7	30.5	+70.5
100	8.92	+22.5	27	+64.5
95	6.8	+18.4	23.8	+60
90	5.5	+14.75	20.5	+56
85	4.6	+11.75	18.8	+52.5
80	4.0	+ 9.1	16.8	+48.5
75	3.5	+ 6.7	15	+45.5

CHART VIII

ℓ = 13 cm. with 5 in. x 5 in. copper plate soldered to the bare center conductor at the end of the antenna
water temperature ~ 21°C
water conductivity ~ 7 mhos/m
line length determined from Chart V

f MC	G Millimhos	B Millimhos	R Ohms	X Ohms
125	51.2	+62	35	+90
120	28	+49.2	31	+82
115	18	+39.3	29.5	+75.9
110	12	+31.6	25.5	+70.3
105	8.8	+25.5	22.8	+65
100	6.75	+20.9	20	+60
95	5.25	+17	18	+57
90	4.3	+13.5	15.5	+52.5
85	3.6	+10.7	14.0	+48.5
80	3.1	+ 8.2	12.3	+46.0
75	2.8	+ 5.8	11.3	+42.3

CHART IX

ℓ = 13 cm. with both plates soldered in place
water temperature ~ 21°C
water conductivity ~ 7 mhos/m
line length determined from Chart V

f MC	G Millimhos	B Millimhos	R Ohms	X Ohms
125	49.2	+57	36.5	+86.5
120	28	+47	32.5	+80
115	17.4	+37.7	28.8	+73
110	12	+30.4	25.5	+68
105	8.62	+24.9	22.5	+64
100	6.39	+20.7	19	+60
95	5	+16.55	17	+56
90	3.97	+13.2	14.3	+51
85	3.4	+10.47	13	+48
80	2.77	+ 7.9	10.5	+44.5
75	2.5	+ 5.54	10	+41.8

Calculated Values of Input Impedance

Assumed water conductivity 9.6 mhos/meter

	CHART X ℓ = 7 cm.		CHART XI ℓ = 9 cm.	
f	R	X	R	X
70	5.047	21.94	6.668	28.58
75	5.439	23.33	7.210	30.46
80	5.837	24.73	7.765	32.33
85	6.241	26.12	8.333	34.22
90	6.651	27.51	8.916	36.11
95	7.069	28.91	9.514	38.02
100	7.494	30.30	10.12	39.94
105	7.927	31.69	10.75	41.86
110	8.368	33.09	11.40	43.81
115	8.817	34.49	12.06	45.77
120	9.275	35.90	12.75	47.75
125	9.742	37.31	13.45	49.75
130	10.21	38.72	14.17	51.76

	CHART XII ℓ = 11 cm.		CHART XIII ℓ = 13 cm.	
f	R	X	R	X
70	8.421	35.51	10.33	42.77
75	9.143	37.91	11.27	45.79
80	9.888	40.34	12.25	48.84
85	10.65	42.79	13.26	51.95
90	11.45	45.27	14.32	55.10
95	12.27	47.77	15.43	58.31
100	13.13	50.31	16.58	61.58
105	14.01	52.87	17.78	64.91
110	14.92	55.48	19.03	68.30
115	15.87	58.12	20.34	71.77
120	16.84	60.80	21.70	75.31
125	17.86	63.52	23.12	78.92
130	18.91	66.29	24.60	82.62

Calculated Values of Input Impedance

Assumed Water Conductivity 9.6 mhos/meter

CHART XIV

ℓ = 15 cm.

f	R	X
70	12.44	50.45
75	13.64	54.15
80	14.89	57.93
85	16.21	61.79
90	17.59	65.73
95	19.04	69.77
100	20.57	73.91
105	22.17	78.15
110	23.85	82.50
115	25.61	86.96
120	27.45	91.55
125	29.38	96.25
130	31.41	101.09

APPENDIX B

Derivation of the Input Impedance of the Modeled Coaxial Antenna

Beginning with (2-53) on page 17

$$Z_{sc} = \frac{\ln \frac{b}{a}\,\Gamma}{j2\pi\omega\epsilon} \tanh \Gamma\ell \ . \tag{B-1}$$

where

$$\Gamma = \sqrt{\frac{\omega^2\mu\epsilon}{\ln \frac{b}{a}} \left[- \ln \frac{2b}{a\gamma |k_B b|} + j\frac{\pi}{4} \right]} \tag{B-2a}$$

by equation (2-49). Rewriting (B-2a)

$$\Gamma^2 = \frac{\omega^2\mu\epsilon}{\ln \frac{b}{a}} \left[- (.1159 - \ln \sqrt{\omega\mu\sigma}\ b) - \ln \frac{b}{a} + j\frac{\pi}{4} \right] . \tag{B-2b}$$

Now the tanh $\Gamma\ell$ is expanded:

$$\tanh \Gamma\ell = \left[\Gamma\ell - \frac{(\Gamma\ell)^3}{3} + \frac{2}{15}(\Gamma\ell)^5 - \frac{17}{315}(\Gamma\ell)^7 + \frac{62}{2835}(\Gamma\ell)^9 - \ldots . \right] . \tag{B-3}$$

Using these five terms in (B-1):

$$Z_{sc} = \frac{\Gamma^2\ell \ln \frac{b}{a}}{j2\pi\omega\epsilon} - \frac{\Gamma^4\ell^3 \ln \frac{b}{a}}{j6\pi\omega\epsilon} + \frac{2\Gamma^6\ell^5 \ln \frac{b}{a}}{j30\pi\omega\epsilon} - \frac{17\Gamma^8\ell^7 \ln \frac{b}{a}}{j(315)(2\pi\omega\epsilon)}$$

$$+ \frac{62\Gamma^{10}\ell^9 \ln \frac{b}{a}}{(2835)(j2\pi\omega\epsilon)} . \tag{B-4}$$

The physical constants which apply to the modeled undersea coaxial antenna are:

$\mu = 4\pi \times 10^{-7}$ henry/meter

$\sigma = 9.6$ mhos/meter

$b = 1.475$ millimeter

$a = .455$ millimeter

$\ln \frac{b}{a} = 1.175$

$\epsilon = 1.857 \times 10^{-11}$ farads/meter.

Using these constants in the bracketed portion of (B-2b) and letting f be the frequency in mc:

$$\Gamma^2 = \frac{\omega^2 \mu \epsilon}{\ln \frac{b}{a}} \left[-.1159 + \ln(\sqrt{2\pi f(.4\pi)(9.6)}\ 1.475 \times 10^{-3}) - 1.175 + j\frac{\pi}{2} \right]$$

$$= \frac{\omega^2 \mu \epsilon}{\ln \frac{b}{a}} \left[-5.6149 + \frac{\ln f}{2} + j\frac{\pi}{4} \right] . \qquad \text{(B-5)}$$

Substituting this into (B-4):

$$Z_{sc} = \frac{-j\omega\mu\ell}{2\pi} \left[-5.6149 + \frac{\ln f}{2} + j\frac{\pi}{4} \right]$$
$$+ \frac{j\omega^3 \mu^2 \epsilon\, \ell^3}{6\pi \ln \frac{b}{a}} \left[-5.6149 + \frac{\ln f}{2} + j\frac{\pi}{4} \right]^2$$
$$- \frac{j\omega^5 \mu^3 \epsilon^2 \ell^5}{(\ln \frac{b}{a})^2 15\pi} \left[-5.6149 + \frac{\ln f}{2} + j\frac{\pi}{4} \right]^3$$
$$+ \frac{j17\omega^7 \mu^4 \epsilon^3 \ell^7}{(315)(2\pi)(\ln \frac{b}{a})^3} \left[-5.6149 + \frac{\ln f}{2} + j\frac{\pi}{4} \right]^4$$
$$- \frac{j62\omega^9 \mu^5 \epsilon^4 \ell^9}{(2835)(2\pi)(\ln \frac{b}{a})^4} \left[-5.6149 + \frac{\ln f}{2} + j\frac{\pi}{4} \right]^5 .$$

Substituting and combining the remaining constants:

$$Z_{sc} = - j\ 1.25663\ (f\ell)\left[- 5.6149 + \frac{\ln f}{2} + j\frac{\pi}{4}\right]$$
$$+ j\ 3.28421 \times 10^{-4}(f\ell)^3\left[-5.6149 + \frac{\ln f}{2} + j\frac{\pi}{4}\right]^2$$
$$- j\ 1.029879 \times 10^{-7}(f\ell)^5\left[-5.6149 + \frac{\ln f}{2} + j\frac{\pi}{4}\right]^3$$
$$+ j\ 3.269113 \times 10^{-11}(f\ell)^7\left[-5.6149 + \frac{\ln f}{2} + j\frac{\pi}{4}\right]^4$$
$$- j\ 1.038539 \times 10^{-14}(f\ell)^9\left[-5.6149 + \frac{\ln f}{2} + j\frac{\pi}{4}\right]^5.$$

This is the expression for the coaxial antenna feedpoint impedance as programmed on the computer. The values of f and ℓ were varied from 70 mc to 130 mc and 7 cm to 15 cm, respectively.

REFERENCES

1. Norgorden, Oscar, The submerged reception of radio frequency signals, NRL Report R-1669, (Washington, D. C., December 2, 1940).

2. Quinn, R. B., and Oscar Norgorden, NRL Report No. 3006, November 6, 1946, (Classified).

3. Tai, C. T., Radiation of a Hertzian dipole immersed in a dissipative medium, Cruft Laboratory Technical Report No. 21, (Harvard University, Cambridge, Mass., October 10, 1947).

4. Moore, R. K., The theory of radio communication between submerged submarines, Ph. D. Thesis (Cornell University, June, 1951).

5. Lien, Roy Harold, Radiation from a horizontal dipole in a Semi-infinite dissipative medium, Journal of Applied Physics, Vol. 24, No. 1, (January, 1953).

6. Baños, A., Jr., and J. P. Wesley, The horizontal dipole in a conducting half space, University of California Marine Physical Laboratory, Reports No. 53-33 (1953) and No. 54-33 (1954).

7. Wait, J. R., The magnetic dipole antenna immersed in a conducting medium, Proc. I.R.E. 40, No. 10, 1244-5, (1952).

8. Wait, J. R., The electromagnetic fields of a horizontal dipole in the presence of a conducting half-space, Canadian Journal of Physics, Vol. 39, No. 7, (July, 1961), p. 1071.

9. King, Ronold W. P., Dipoles in dissipative media, Cruft Laboratory Technical Report No. 336, p. 1-2, (Harvard, February, 1960).

10. Kraichman, M. R., Basic experimental studies of the magnetic field from electromagnetic sources immersed in a semi-infinite conducting medium, Journal of Research NBS 64D, No. 6, p. 21, (January, 1960).

11. Saran, G. S., and G. Held, Field strength measurements in fresh water, Journal of Research NBS 64D, (Radio Propagation), No. 5, 435-7, (September, 1960).

12. Flath, Earl H., and Oscar Norgorden, Expressions for input impedance and power dissipation in lossy concentric lines, NRL Report R-3436, (Washington, D. C., March 24, 1949).

13. Anderson, Wallace L., The fields of electric dipoles in sea water, the earth-air-ionosphere problem, University of New Mexico, Technical Report EE-44, (Albuquerque, February, 1961).

14. Anderson, Wallace L., Submerged antennas, University of New Mexico, Technical Memorandum No. 2, (Albuquerque, June 12, 1961).

15. Williams, Richard H., Propagation between conducting and nonconducting media, University of New Mexico, Technical Report EE-50, (Albuquerque, Sept., 1961).

16. Moore, R. K., and W. E. Blair, Vertical and horizontal, electric and magnetic dipole radiation in a conducting half space, University of New Mexico, Technical Report No. EE-40, (Albuquerque, January, 1961).

17. Stratton, J. A., Electromagnetic theory, McGraw-Hill Book Company, Inc., (New York and London, 1961).

18. Schelkunoff, S. A., Electromagnetic waves, D. Van Nostrand Company, Inc., (New York: 1943).

19. Jahnke, Eugene, and Fritz Emde, Table of functions, Dover Publications, (New York: 1945).

20. Dwight, Herbert B., Tables of integrals and other mathematical data, Macmillan Co.,(New York: 1961).

21. Thomas, George B., Calculus, pp. 432-435, Addison Wesley, (Reading, Mass.: 1956).

DISTRIBUTION LIST FOR UNCLASSIFIED REPORTS

CONTRACT Nonr 2798(01)

Addressee	No. of Copies
Director Armed Services Technical Information Agency Arlington Hall Station, Arlington, Virginia	10
Chief of Naval Research Code 466 Code 427 Washington 25, D. C.	3 1
Director Special Projects (SP204) Bureau of Naval Weapons Washington 25, D. C.	25
Commanding Officer Office of Naval Research Branch Office 1030 East Green Street Pasadena 1, California	3
Chief of Naval Operations Op 07 Op 94T Washington 25, D. C.	1 2
Chief of Bureau of Ships Navy Department Code 671C Code 679 Code 686 Code 687H Code 687A Washington 25, D. C.	 1 1 1 1 1
Director, Naval Research Laboratory Code 5360 Code 5420 Code 2027 Code 5423 (Attention: Mr. L. S. Bearce) Washington 25, D. C.	 1 1 3 1
Commanding Officer and Director U. S. Navy Underwater Sound Laboratory Fort Trumbull New London, Conn. Attn: Mr. G. M. Milligan	1

Dr. L. Katz
Applied Physics Laboratory
Johns Hopkins University
Silver Spring, Maryland 1

Director
Research Laboratory of Electronics
Mass. Institute of Technology
Cambridge 39, Mass. 1

Dr. R. W. P. King
Cruft Laboratory
Harvard University
Cambridge 38, Mass. 1

Electrical Engineering Research
Document File
School of Electrical Engineering
Cornell University
Ithaca, New York 1

University of Chicago
Laboratories for Applied Science
Museum of Science
Chicago 37, Ill.
Attn: Mr. Van Zeelind 1

Director Hudson Laboratories
Columbia University
P. O. Box 329
Dobbs Ferry, New York 1

Dr. J. H. Mulligan, Jr.
Chairman, EE Dept.
New York University
New York 53, N. Y. 1

Dr. B. M. Fannin
Electrical Engineering Research Laboratory
University of Texas
Austin 3, Texas 1

Ordnance Research Laboratory
Pennsylvania State College
P. O. Box 30
State College, Pa. 1

Dr. R. H. Duncan
Physical Science Laboratory
New Mexico State University
University Park
Las Cruces, New Mexico 1

University of New Mexico
EE Dept. 1

Mr. Albert R. Giddis
Project Engineer
Advance Programs Section
Philco Corporation
Western Development Laboratory
3875 Fabian Way
Palo Alto, Calif. 1

Dr. Ronald V. Row
Sylvania Electronic Systems
Division of Sylvania Electric
Products, Inc.
100 First Ave.
Waltham 54, Massachusetts 1

Development Engineering Co.
Attn: Mr. Don Watt
Boulder, Colorado 1

Development Engineering Co.
Attn: Mr. Lucien Rawls
Leesburg, Virginia 1

Space Electronics Corp.
1200 AirWay
Glendale 1, California
Attn: Mr. Frank W. Lehan 1

Mr. Harold A. Wheeler
Wheeler Laboratories, Inc.
122 Cutter Miller Road
Great Neck, N. Y. 1

Stromberg-Carlson
Division of General Dynamics
Rochester, N. Y.
Attn: Victor Savchuk 1

Mr. Martin Katzin
Electromagentic Research Corp.
5001 College Avenue
College Park, Maryland 1

Mr. Walter N. Phillips
Research Division
Electronics Communications, Inc.
1830 York Road
Timonium, Maryland 1

Mr. Richard C. Becker
Senior Staff Engineer
Amphenol-Borg Electronics Corp.
25th Avenue at Cermak
Broadview, Ill. 1

National Research Council
Committee on Undersea Warfare
2101 Constitution Ave., NW
Washington 25, D. C. 1

Dr. J. R. Wait, Consultant
Central Radio Propagation Laboratory
National Bureau of Standards
Boulder, Colorado 2

Mr. Kenneth A. Norton, Chief
Radio Propagation Engineering Division
Central Radio Propagation Laboratory
National Bureau of Standards
Boulder, Colorado 1

Dr. Cullen Crain
Rand Corporation
Santa Monica, California 1

Director
Woods Hole Oceanographic Institution
Woods Hole, Mass.
Attn: Dr. Hersey 1

Director
Scripps Institution of Oceanography
La Jolla, Calif. 1

Mr. J. Y. Wong
Antenna Group (Microwave Section)
National Research Council of Canada
Ottawa 2, Ontario, Canada 1

Stanford Electronics Laboratories
Stanford University
Stanford, California 1

Stanford Research Institute
Menlo Park, California
Attn: Mr. Geo. H. Hagn 1

Mr. L. H. Rorden
Stanford Research Institute
Menlo Park, California 1

Applied Physics Laboratory
Johns Hopkins University
Attn: Cdr. Pollow
8621 Georgia Avenue
Silver Spring, Maryland 1

Commanding Officer and Director
U. S. Naval Ordnance Laboratory
Corona, Calif.
Attn: Mr. A. W. Walters
Code 45 1

Technical Director
U. S. Naval Ordnance Test Station
China Lake, Calif. 1

Commanding Officer and Director
U. S. Naval Ordnance Laboratory
White Oak, Maryland
Attn: Mr. Robert J. Miller
Code 042 1

Commander
U. S. Naval Ordnance Test Station
3202 East Foothill Blvd.
Pasadena 8, California 1

Commanding Officer and Director
U. S. Navy Underwater Sound Laboratory
New London, Conn.
Attn: Mr. C. B. Dunn 2

Commanding Officer and Director
Naval Electronics Laboratory
San Diego 52, California 1

Commanding Officer and Director
U. S. Navy Mine Defense Laboratory
Panama City, Florida
Attn: Code 710 1

Mr. Martin G. Kraichman
Naval Ordnance Laboratory
White Oak, Maryland 1

Commanding General
White Sands Missile Range
New Mexico
Attn: Technical Library RR-162 1

Program Director
Advanced Science Programs
National Science Foundation
1951 Constitution Ave.,
Washington 25, D. C. 1

National Science Foundation
Engineering Program
Washington 25, D. C. 1